Hindawi Publishing Corporation
Advances in Materials Science and Engineering
Volume 2013, Article ID 149261, 8 pages
http://dx.doi.org/10.1155/2013/149261

Research Article

Physicochemical and Microstructural Characterization of Injectable Load-Bearing Calcium Phosphate Scaffold

Mazen Alshaaer,[1,2] Mohammed H. Kailani,[1,3] Hanan Jafar,[1,4] Nidaa Ababneh,[1] and Abdalla Awidi[1,4]

[1] *Cell Therapy Center (CTC), The University of Jordan, Amman 11942, Jordan*
[2] *Department of Physics, College of Science and Humanitarian Studies, Salman Bin Abdul Aziz University, P.O. Box 83, Alkharj 11942, Saudi Arabia*
[3] *Department of Chemistry, The University of Jordan, Amman 11942, Jordan*
[4] *Faculty of Medicine, The University of Jordan, Amman 11942, Jordan*

Correspondence should be addressed to Mazen Alshaaer; mazen72@yahoo.com

Received 20 July 2013; Revised 19 October 2013; Accepted 30 October 2013

Academic Editor: Wei Wu

Injectable load-bearing calcium phosphate scaffolds are synthesized using rod-like mannitol grains as porogen. These degradable injectable strong porous scaffolds, prepared by calcium phosphate cement, could represent a valid solution to achieve adequate porosity requirements while providing adequate support in load-bearing applications. The proposed process for preparing porous injectable scaffolds is as quick and versatile as conventional technologies. Using this method, porous CDHA-based calcium phosphate scaffolds with macropores sizes ranging from 70 to 300 μm, micropores ranging from 5 to 30 μm, and 30% open macroporosity were prepared. The setting time of the prepared scaffolds was 15 minutes. Also their compressive strength and e-modulus, 4.9 MPa and 400 MPa, respectively, were comparable with those of the cancellous bone. Finally, the bioactivity of the scaffolds was confirmed by cell growth with cytoplasmic extensions in the scaffolds in culture, demonstrating that the scaffold has a potential for MSC seeding and growth architecture. This combination of an interconnected macroporous structure with pore size suitable for the promotion of cell seeding and proliferation, plus adequate mechanical features, represents a porous scaffold which is a promising candidate for bone tissue engineering.

1. Introduction

Bone defects arise from skeletal diseases, congenital malformations, trauma, and tumor resection [1, 2]. The need for bone reconstruction is increasing as the population ages. Tissue engineering approaches are promising alternatives to autogenous bone grafts. Studies have shown exciting results on the use of scaffolds and stem cells for tissue regeneration [3–7]. Human mesenchymal stem cells (MSCs) can differentiate into adipocytes, osteoblasts, chondrocytes, neurons, endothelial cells, and so forth [8–12]. Scaffolds can serve as templates for cell attachment, differentiation, and vascularization *in vivo* and can then degrade and be replaced by new bone. Calcium phosphate (CaP) scaffolds mimic the bone mineral and can bond to bone to form a functional interface [13–16]. Preformed CaP implants require machining to fit into a bone cavity. In contrast, calcium phosphate cements can be injected or sculpted and set *in situ* to form a scaffold with intimate adaptation to the neighboring bone [17–21]. Due to its similarity to the mineral phase of the bone, good biocompatibility, excellent bioactivity, self-setting characteristics, low setting temperature, adequate stiffness, and easy shaping in complicated geometrics, calcium phosphate cement (CPC) is regarded as a promising material for use in minimally invasive surgery to repair bone defects [22–25]. Because CPCs are osteotransductive, after implantation in bone defects they are rapidly integrated into the bone structure and transformed into new bone by the cellular activity of osteoclasts and osteoblasts in local bone remodeling [24]. A major disadvantage of current orthopedic implants is that they are hard, requiring the surgeon to fit the surgical site around the implant or to carve the graft

to the desired shape. This can lead to increased bone loss, trauma to the surrounding tissue, and prolonged surgical time [23]. However, CPCs typically set at low temperatures following the combination of a solid component containing one or several calcium orthophosphate salts and an aqueous solution and form a solid calcium phosphate *in situ*. This means that CPCs can adapt immediately to each bone cavity and obtain good osteointegration. In addition, injectable CPC formulations that are suitable for new minimally invasive surgical techniques have been developed [26]. In the last two decades, numerous biomaterials studies have been conducted investigating the development of CPCs. However, the physicochemical characterization and *in vitro* evaluation of the final properties of CPCs produced from calcium pyrophosphate powder have not been studied systematically. In this study, the main reactive ingredient of CPC, tetracalcium phosphate (TTCP, $Ca_4(PO_4)_2O$), was synthesized by solid state reaction between calcium pyrophosphate (CaPyro, $Ca_2P_2O_7$) and calcium carbonate ($CaCO_3$). The aim of this work consists in designing an injectable and strong porous system using biocompatible materials able to promote natural body healing, which degrade after implantation and contain biologically active phases, and able to stimulate the regenerative tissue growth in order to mimic the morphological and microstructural properties of bone tissue. We investigated the microstructural properties, phase evaluation, pore structure, densities, compressive strength, and stiffness of the produced scaffolds. We also evaluated the bone formation properties and cell differentiation *in vitro* over a time scale of 21 days.

2. Materials and Methods

2.1. Synthesis of TTCP. The TTCP powder used for this study was fabricated from the reaction of dicalcium pyrophosphate ($Ca_2P_2O_7$) (Merck, Germany) and calcium carbonate ($CaCO_3$) (Merck, Germany) with a weight ratio of 1 : 1.27. The powders were mixed uniformly in ethanol for 12 h. Then the mixed powder was dried and crushed using a mortar and a pestle, followed by calcination in a crucible at 1500°C for 5 h in air and quenching in air at 25°C. Finally the calcined powder (TTCP phase) was ground into a fine powder.

The chemical reaction for the TTCP powder was as follows:

$$Ca_2P_2O_7 + 2CaCO_3 \longrightarrow Ca_4(PO_4)_2O\,(\text{TTCP}) + 2CO_2 \quad (1)$$

2.2. Fabrication of the Macroporous CPC Scaffold. Water-soluble granular rod-like mannitol porogen was incorporated into CPC to create macropores. The TTCP powder was mixed with granulated mannitol with size that varies from 70 μm to 300 μm (mannitol/TTCP weight ratio is 0.5). This mixture was then mixed in diammonium hydrogen phosphate ($(NH_4)_2HPO_4$, 33.3 wt%) with hardening solution/TTCP ratio of 0.34 mL/g. After mixing the CPC for 1 min, the cement paste was uniformly packed in a polymer mold which has an opening of 10 × 10 mm and 3 mm in depth under a pressure of ~1.4 MPa at 37°C. The hardened CPC was then removed from the mold and immersed in Hanks' physiological solution at 37°C for 2 days to dissolve the mannitol.

2.3. CPC Setting Time. The CPC setting time was measured using a previously reported method [27]. The CPC paste was placed in a 3 × 4 × 25 mm mold and placed in a humidified atmosphere at 37°C. At 1 min intervals the specimen was scrubbed gently with fingers until the powder component did not come off. This indicated that the setting reaction had occurred to a sufficient extent to hold the specimen together. The time from powder-liquid mixing to this point was measured as the setting time.

2.4. Microstructural Characterization of Scaffolds

2.4.1. Scanning Electron Microscopy. An Inspect F50 scanning electron microscopy was used to examine the specimens. The MSCs attached to the scaffolds were rinsed twice with 2 mL of 1X PBS and fixed with a 2% glutaraldehyde for 24 h at 4°C. Samples were then subjected to graded alcohol dehydrations, air-dried using filter papers, sputter-coated with platinum, and viewed by SEM. Matrices without cells were used as controls.

2.4.2. X-Ray Diffraction (XRD). XRD was used to identify the crystallographic phases of the reaction products such as the TTCP powder, the set CPC, and the sintered CPC. For the XRD analysis, the samples were ground into fine powders and each powder was mounted in a specimen holder for the diffractometer (Shimadzu XRD-6000 using CuKα radiation at 20 mA, 40 kV). Scans were performed from 5° to 80° at a rate of 2°/min.

2.5. Physical Characterization of Scaffolds

2.5.1. Open Porosity and Pore Structure Analysis. Pore structure and open porosity/pores interconnection (1–400 microns) were calculated by MIP (mercury intrusion porosimetry), that is, differential mercury intrusion volume related to the applied pressure. A PoreMaster (USA) was used for mercury intrusion porosimetry test. The samples were placed in a closed cell called penetrometer and evacuated. Applying high pressure via mercury intrusion porosimetry could damage the structure of the pores [28]. Therefore pore structure of the samples was characterized only by applying low vacuum level. After reaching this low vacuum level (~ 3 kPa), the cell was filled with mercury and pressure was increased continuously to 0.3 MPa. The surface tension was 480 erg/cm^2 and the contact angle was 140°.

2.5.2. Skeletal Density. Helium pycnometry is a technique used to determine the true density of solids. Since helium can enter the smallest voids or pores, the density obtained is often referred to as skeletal density (ρo). It is measured with a helium pycnometer, specifically Micromeritics AccuPyc 1330 He pycnometer. The measurements of skeletal density were performed as follows: helium was first loaded in

a calibrated reference volume and then expanded in a chamber filled with the sample. The change of pressure of the helium in the known cell volume without and with the specimen means that the volume of the specimen's mineral matrix can be determined. Dividing the mass of the specimen by this volume yields the true density. Four samples were prepared for measuring the variations of skeletal density (by using helium pycnometry) as a function of temperature. The volume of each of them is around 6 cm^3. The samples were crushed into small aggregates. Afterward, they were heated for 24 hours at 10°C before testing. The specimens were put immediately in the testing chamber to avoid any moisture uptake.

2.5.3. Total Porosity. The total porosity of the sintered porous CPC sample was determined using the following equations:

$$\rho B = \frac{m}{V}, \tag{2}$$

where ρB, m, and V refer to bulk density, mass of the sample, and volume of the sample respectively.

$$RD = \frac{\rho B}{\rho o} \times 100\%, \tag{3}$$

where RD is the relative density and ρo is the skeletal density for solid fraction (ρo) obtained by helium pycnometry.

$$\text{Total porosity} = 100\% - RD. \tag{4}$$

The dimensions and the weight of each sample were measured and recorded through a vernier caliper and an electronic balance, respectively.

2.6. Compressive Test and Young's Modulus. For the measurements of the compressive strength of the porous samples, rubber pads were placed on the top and the bottom surfaces of each sample [13]. The rubber padded sample was then placed in a CBR tester (controls) to conduct a compressive test. The rubber pads were used to ensure a uniform distribution of the applied load onto the sample. A crosshead speed of 0.4 mm/min was used for the compressive tests.

In the material's stress-strain curve, there is a linear region where the material follows Hooke's law. Hence the following equation stands for this region:

$$\sigma = E\varepsilon, \tag{5}$$

where E refers to Young's modulus for compression and ε is the strain caused by the compressive stress.

2.7. In Vitro Characterisation of Scaffolds

2.7.1. MSCs Cell Isolation. MSCs were isolated from human bone marrow aspirates via density gradient centrifugation. The cells were expanded in nondifferentiating MSC growth medium (CCM) consisting of α-minimal essential medium (α-MEM) with 10% foetal bovine serum (FBS), 1% penicillin-streptomycin (PEN-STREP), and 2 mM glutamine. Cells were incubated at 37°C with 5% CO_2. After they reached 90% confluence, cells were harvested by rinsing with 0.25% trypsin and 0.03% EDTA solution and expanded into a second passage until they reached 80% confluence, then they were trypsinized and cryopreserved in a liquid nitrogen. These cells were designated as passage 1 (P1) cells.

2.7.2. Osteogenic Differentiation. Cells were seeded in 12 multiwell plates for an estimated 80% confluence. Each experiment comprised 12 cultures, 6 under osteogenic conditions and 6 controls under normal cell cultures conditions (CCM). To induce the osteogenic differentiation of the MSCs, the cultures were maintained in osteogenic media which consist of 60 μM ascorbic acid, 10 mM β-glycerol phosphate, and 100 nM dexamethasone. The medium was changed every 2-3 days.

2.7.3. Cells Seeding on the Bioceramic Scaffolds. Cryopreserved (P1) cells were replated at a seeding density of 4,000 cells/cm^2 in α-MEM as described above. At near confluency, P2 cells were harvested with 0.25% trypsin in EDTA and resuspended at a density of 2×10^5 cells/mL α-MEM plus 1% penicillin/streptomycin. The calcium phosphate scaffolds were sterilized in 70% ethanol for 24 h and then incubated with cell culture media containing 10% FBS for at least 4 h. Then the MSCs were seeded into the scaffolds with a cell seeding density of 200,000 cells per scaffold. The MSCs were cultured with osteogenic medium and cell culture medium as a standard control to verify their proliferative and differentiation potential at 37°C and 5% CO_2. The medium was changed every 3 or 4 days.

3. Results and Discussion

3.1. Microstructural, Morphological, and Physical Characterization. The aim of this work is designing an injectable and strong porous system using biocompatible materials able to promote natural body healing, which degrade after implantation and contain biologically active phases, and able to stimulate the regenerative tissue growth in order to mimic the morphological and microstructural properties of bone tissue. The starting material of the prepared scaffolds is tetracalcium phosphate (TTCP, $Ca_4(PO_4)_2O$). The analysis of the XRD diffraction peaks (Figure 1 lower pattern) revealed that the TTCP was formed as the main phase of CPC powder by firing the mixture of pyrocalcium phosphate ($Ca_2P_2O_7$) and calcium carbonate ($CaCO_3$) at 1500°C for 5 h, followed by quenching in air. Moreover, this CPC powder contained a few peaks corresponding to HA. The peaks in the lower XRD pattern are strong and sharp, which indicate relatively high crystallinity of the powder. The setting time of the CPC was around 15 min.

After seting CPC, while the hydroxyapatite phase was present in the form of intensive layer of nano-HA crystals as shown by the SEM image, Figure 2(c), some residual TTCP were still left behind, Figure 1 (XRD upper pattern). In addition, the residual TTCP phase was depleted to a great extent for the formation of hydroxyapatite due to the

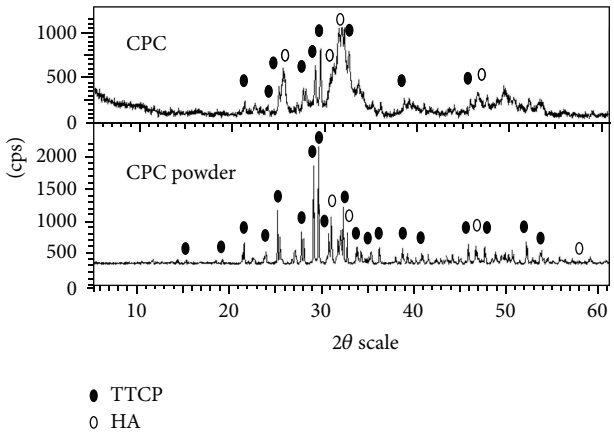

Figure 1: XRD patterns of CPC powder (tetracalcium phosphate, TTCP) and hardened CPC (1 day after mixing with the hardening solution to form calcium phosphate cement). HA is hydroxyapatite.

setting reactions to form calcium phosphate cement (CPC). The high backgrounds of the upper XRD pattern (Figure 1) between 30° and 35° and 45° and 55° indicate the presence of amorphous or poorly crystalline CaP phase, mainly CDHA (Calcium-deficient HA), as shown by the EDS measurements with Ca/P ratio of 1.6.

The SEM micrographs of the fabricated scaffold taken at different magnifications are reported in Figure 2. To discuss these morphologies, it is important to define three types of pores: fine pores, micropores, and macropores. These pores are distinguished by their size: fine pores have a diameter below 5 μm and micropores have a diameter typically close to the range of 5–30 μm, whereas macropores have a diameter above 70 μm. The threshold is placed at a size of 50 mm. The rod-like mannitol particles were thus used only as a template to form the scaffold framework with the desired pore structure for bone tissue engineering applications. This open internal pore network is necessary to maximize nutrient diffusion, interstitial fluid, and blood flow, to control cell growth and function, to manipulate tissue differentiation, and to optimize scaffold mechanical function and regenerated tissue mechanical properties [29]. Another feature of the porous CPC was the presence of well-connected macropores, with diameters between 70 μm and 300 μm inside the struts as shown in Figure 2(a). The CPC contained mainly calcium-deficient hydroxyapatite phase with macropores (as a replica of the dissolved rod-like mannitol particles) in the overall structure and open micropores in the struts as shown in Figure 2(b). This design of injectable scaffolds with well-connected pores, or highly effective porosity, intended to favor an increase in the mass transport of nutrients and oxygen, and removal of waste products for cell growth.

In the presence of hardening phosphate solution, TTCP hydrolyses through a dissolution precipitation reaction giving rise to the formation of an entangled network of CDHA crystals, which are close to the mineral component of the bone from a structural point of view. In the proposed scaffolds, the hydrolysis reaction occurs during the setting of the bone cement. This is confirmed by XRD and SEM (Figures 1 and 2(c)), which show a large distribution of CDHA needle-like crystals approximately 1 μm long and homogeneously distributed along the inner surface pores (Figure 2(c)). These do not significantly affect the scaffold porosity in terms of pore shape and interconnection degree [14]. Several works have demonstrated the feasibility of forming new bone in close contact with calcium-deficient apatite (CDHA) granules. This creates a network of woven bone bonded to residual calcium phosphate particles, as confirmed by no adverse inflammatory reactions and formation of multinucleated giant cells close to the CDHA granules [16].

To confirm the qualitative morphological evaluation performed by SEM, a quantitative estimation of porosity characteristics was performed by mercury intrusion porosimetry (MIP). The pore size distribution and final open pore volume of representative scaffolds were characterized by low pressure (to avoid damage of pore structure) mercury intrusion porosimetry (MIP) [28, 30] (Figure 3). Pore interconnectivity first arises by the dissolved mannitol grains and the contact point between adjacent grains, Figure 2(b), also due to the presence of smaller pores (up to 30 μm) induced by the phase conversion mechanism [14]. Fine pores network can be observed within these channel walls as shown in Figure 2(c).

MIP showed evidence of a bimodal distribution of pore size with diameter above 5 μm. This pore structure is characterized by micropores a few micrometers in diameter and macropores of the order of hundreds micrometers (see also Figure 2(a)). It is apparent that the total open micropore and macropore volume is nearly 30% of the scaffold volume, Figure 3. The calculations and measurements of volume, weight, and bulk density show that the total porosity is around 64%. It was possible to observe, Figure 2(b), the characteristic sizes of the smaller pores (with diameters ranging from 5 to 30 μm (microporosity)), peak A, and of larger pores, peak B, (with diameters ranging from ~70 to ~300 μm (macroporosity)). The pores with diameter above 5 μm represent around 50% of the total open porosity. In this structure, the macropores are suitable for the accommodation of osteoblast and undifferentiated bone mesenchymal stem cells, while the micropores offer interconnection bridges between adjacent macropores, able to promote the nutrient and metabolite exchange [15–18], improving the structural interconnectivity.

One of the most important requirements of an ideal bone substitute is for it to exhibit mechanical behavior matching that of the bone tissue that has to be restored. The accurate mimesis of specific mechanical properties, such as elastic modulus, may be crucial to the effective reproduction of the functional response of natural tissue, especially in load-bearing applications. In the last decade, the use of polymers such as PLA, PGA, and PCL has been a popular strategy for the provision of biodegradable supports for orthopedic applications [13]. However, their deficient mechanical properties limited their use mainly to a restricted number of non-load-bearing applications [18]. Figure 4 shows the representative stress-strain responses of the fabricated CPC scaffold. This diagram shows that the scaffold exhibits compressive strength of 4.9 MPa. The e-modulus of the scaffold in compression, ~400 MPa, was obtained from the slope of the stress-strain curve.

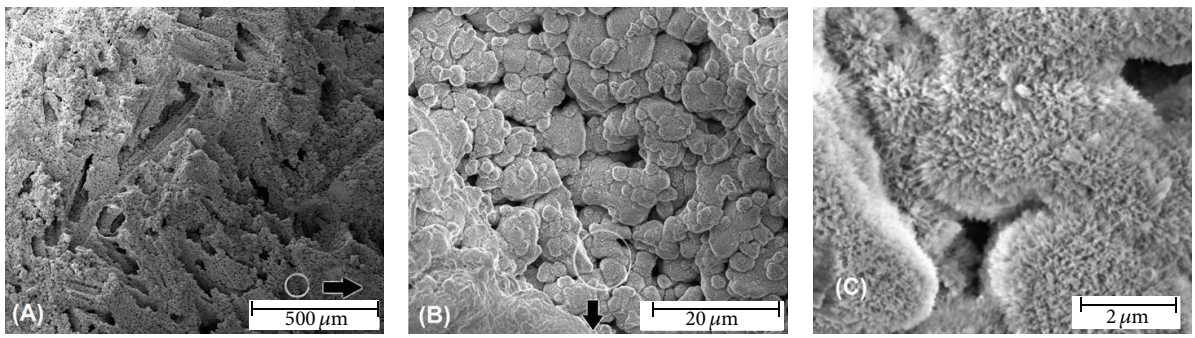

(a) (b) (c)

Figure 2: SEM micrograph of a fracture surface of the porous calcium phosphate scaffold with different magnifications: (a) macropore network, (b) micropore structure of the internal walls of macropore, and (c) matrix of needle-like CDHA (calcium deficient hydroxyapatite) crystals covering the surfaces of the pores.

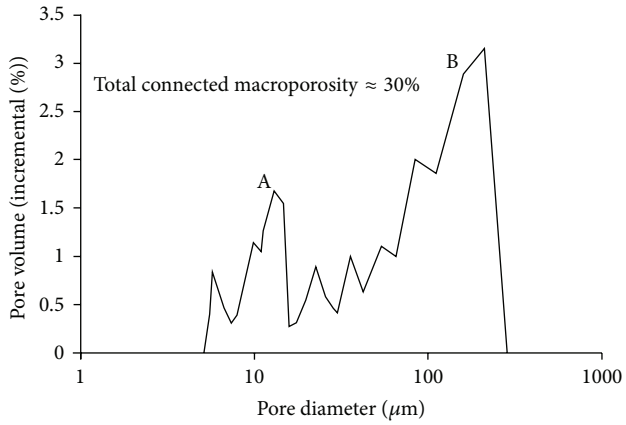

Figure 3: Low pressure mercury intrusion porosimetry of CPC scaffold. Incremental pore size in % above 5 μm.

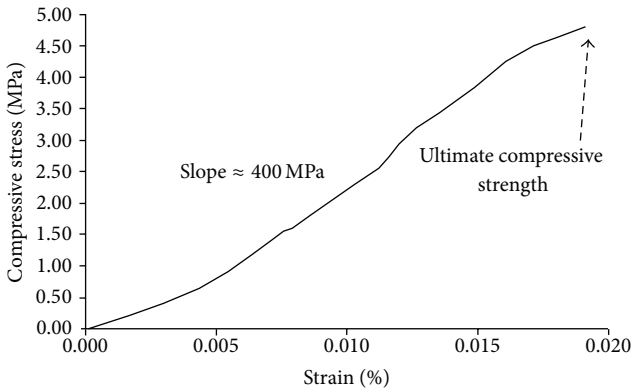

Figure 4: Representative stress-strain responses of the produced scaffold to compression test.

The CPC paste can intimately adapt to complex-shaped bone defects and bond to neighboring bone to form a functional interface. The good mechanical properties, shown in the present study, could enable stem cell delivery to moderate load-bearing repairs. For example, in mandibular and maxillary ridge augmentation, the CPC could be molded to the desired esthetic shape and then set to form a macroporous scaffold containing stem cells for bone regeneration. These implants would be subjected to early loading by provisional dentures. Therefore, the macroporous CPC scaffold needs to be resistant to flexure. In addition, the CPC paste could be used in major reconstructions of the maxilla or mandible after trauma or tumor resection, which would require the CPC to be fracture resistant [30]. The CPC could also be used to support metal dental implants or augment deficient implant sites, where mechanical properties are important. It should be noted that, to repair large defects, mechanical strength is only one factor to consider. Other factors such as vascularization are also critically important for success [31, 32]. The macroporous CPC in the present study possessed better mechanical properties than other injectable carriers for cell delivery. For example, previous studies reported that an injectable polymeric carrier for cell delivery had a strength of 0.7 MPa [33] and hydrogels had strengths of about 0.1 MPa [34, 35]. These systems are promising for non-load-bearing applications. However, their strengths are much lower than the reported strength of about 3.5 MPa for cancellous bone [36]. This macroporous CPC with a strength of 4.9 MPa matched that of cancellous bone and, hence, may be a promising injectable scaffold for stem cell in orthopedic and craniofacial applications. The bulk density of the scaffold is 1.09 g/cm^3 and the total porosity is 64%. The mechanical and physical properties of the scaffold were in a range of those of cancellous bone. Therefore, it is suggested that this scaffold is one of promising scaffold materials for hard tissue regeneration, Table 1.

In the light of recent approaches in bone regeneration, based on composite materials, the proposed strategy certainly offers the best compromise between structural and functional properties. Porous composite scaffolds made by incorporating bioactive particles [37] do not assure an adequate improvement in the mechanical performance for bone substitution. Meanwhile, composites materials formed by integrating high modulus PLA fibers coated with calcium phosphate (CaP) into a PCL matrix [38] show mechanical properties that are significantly higher than the values reported in the literature for PLA-CaP composites but lack

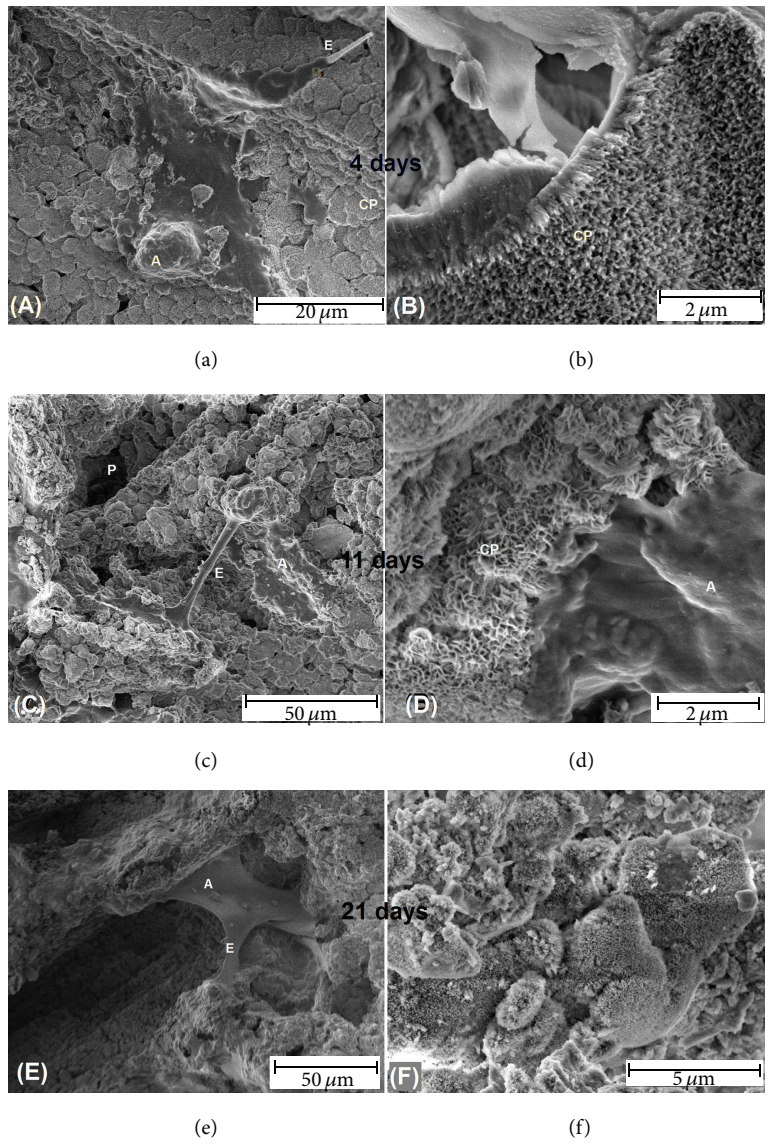

Figure 5: Representative SEM image showing cell attachment to the surface of CPC scaffold with cytoplasmic extensions (e) after culturing for 4, 11, and 21 days—images (a), (c), and (e), respectively. The other 3 images ((b), (d), and (f)) show the development of the calcium phosphate matrix over time.

Table 1: Comparison between the CPC scaffold and cancellous bones [19–21].

Types of materials	Compressive strength (MPa)	Total porosity %	Bulk density (g/cm^3)	Macropore size (μm)	Elastic modulus (GPa)
Bioceramic scaffold	4.9	64	1.09	70–300	0.4
Cancellous bones	0.2–80	30–90	1–1.4	200–400	0.01–2

structural porosity. In contrast, the proposed scaffolds show an intermediate level of mechanical response in porous structure.

3.2. Preliminary Evaluation of Biocompatibility of Scaffolds. The injectable CPC scaffolds were prepared for preliminary *in vitro* cultivation. MSCs were seeded on the 3D scaffolds and maintained with osteogenic medium for 4 days, 11 days, and 21 days. After 3 days of culturing, cells showed no regular orientation and mineralized nodules (A, Figure 5(a)) were formed in the constructs. The size of the cells varies from 20 μm to 40 μm. Figure 5(a) shows that the cells adhered to the CPC and developed cytoplasmic extensions (e). After 4 days, a homogeneous needle-like CDHA matrix covers the internal surfaces of the scaffold, Figure 5(b). After 11 days of culturing, most pores were filled with new tissue mass as

observed by SEM (Figure 5(c)). The CDHA matrices visually demonstrated high cell density on the surfaces of the matrix within the cylindrical macropores as shown in Figures 5(c) and 5(d).

As reported in Figure 5(c), cells attaching to the nano-sized CDHA crystals that make up the scaffold matrix. Cell adhesion resulted in elongated and highly stretched cells within the macropores with focal adhesion points and multicytoplasmic extensions on the scaffolds after 21 days of culturing, (Figure 5(e)). Moreover, cells growth in the scaffolds in culture shows the potential of using this scaffold architecture for MSC seeding and growth. The bone matrix consists of CDHA crystals (Figure 5(f)) containing calcium and phosphorus. Therefore, these factors provide important indicators of osteogenic differentiation.

4. Conclusions

Engineering tissue with cells and a synthetic extracellular matrix is an alternative approach to the established practice of transplantation of harvested tissues. Degradable injectable porous scaffolds, prepared by calcium phosphate cement, represent a valid solution to achieving adequate porosity requirements while providing adequate support in load-bearing applications. This proposed process for preparing injectable scaffolds with two pore networks is as quick and versatile as conventional technologies. Using this method, porous CDHA-based calcium phosphate with macropores sizes ranging from 70 to 300 μm, micropores ranging from 5 to 30 μm, and 30% open macroporosity was prepared. The compressive strength and the e-modulus of the porous hydroxyapatite-based calcium phosphate samples, 4.9 MPa and 400 MPa, respectively, were comparable with those of the cancellous bone. Finally, the bioactivity of the scaffolds was confirmed by cells growth and cytoplasmic extensions in the scaffolds in culture, demonstrating that the scaffold is suitable for MSC seeding and growth architecture. This combination of an interconnected macroporous structure with pore size has a potential for the promotion of cell seeding and proliferation, plus adequate mechanical features, and represents a porous scaffold, which is an excellent candidate for bone tissue engineering with setting time around 15 min.

Acknowledgments

The financial support of the project "Synthesis and characterization of scaffolds for bone tissue engineering" funded by the Deanship of Academic Research at the University of Jordan is gratefully acknowledged. The authors would like to take this opportunity to thank the Hamdi Mango Center for Scientific Research (HMCSR), University of Jordan, for providing the laboratory facilities.

References

[1] J. J. Mao, G. Vunjak-Novakovic, A. G. Mikos, and A. Atala, *Regenerative Medicine: Translational Approaches and Tissue Engineering*, Artech House, Boston, Mass, USA, 2007.

[2] M. Bohner, "Design of ceramic-based cements and putties for bone graft substitution," *European Cells and Materials*, vol. 20, pp. 1–12, 2010.

[3] M.-P. Ginebra, C. Canal, M. Espanol, D. Pastorino, and E. B. Montufar, "Calcium phosphate cements as drug delivery materials," *Advanced Drug Delivery Reviews*, vol. 64, pp. 1090–1010, 2012.

[4] C. S. Che Nor Zarida, O. Fauziah, A. K. Arifah et al., "In vitro elution and dissolution of tobramycin and gentamicin from calcium phosphate," *African Journal of Pharmacy and Pharmacology*, vol. 5, no. 20, pp. 2283–2291, 2011.

[5] J. J. Mao, W. V. Giannobile, J. A. Helms et al., "Craniofacial tissue engineering by stem cells," *Journal of Dental Research*, vol. 85, no. 11, pp. 966–979, 2006.

[6] P. C. Johnson, A. G. Mikos, J. P. Fisher, and J. A. Jansen, "Strategic directions in tissue engineering," *Tissue Engineering*, vol. 13, no. 12, pp. 2827–2837, 2007.

[7] P. Habibovic, U. Gbureck, C. J. Doillon, D. C. Bassett, C. A. van Blitterswijk, and J. E. Barralet, "Osteoconduction and osteoinduction of low-temperature 3D printed bioceramic implants," *Biomaterials*, vol. 29, no. 7, pp. 944–953, 2008.

[8] H. S. Wang, S. C. Hung, S. T. Peng, C. C. Huang, H. M. Wei, Y. J. Guo et al., "Mesenchyma lstem cells in the Wharton's jelly of the human umbilical cord," *Stem Cells*, vol. 22, pp. 1330–1337, 2004.

[9] D. Baksh, R. Yao, and R. S. Tuan, "Comparison of proliferative and multilineage differentiation potential of human mesenchymal stem cells derived from umbilical cord and bone marrow," *Stem Cells*, vol. 25, no. 6, pp. 1384–1392, 2007.

[10] E. Verron, I. Khairoun, J. Guicheux, and J.-M. Bouler, "Calcium phosphate biomaterials as bone drug delivery systems: a review," *Drug Discovery Today*, vol. 15, no. 13-14, pp. 547–552, 2010.

[11] A. Can and S. Karahuseyinoglu, "Concise review: human umbilical cord stroma with regard to the source of fetus-derived stem cells," *Stem Cells*, vol. 25, no. 11, pp. 2886–2895, 2007.

[12] L. Wang, M. Singh, L. F. Bonewald, and M. S. Detamore, "Signalling strategies for osteogenic differentiation of human umbilical cord mesenchymal stromal cells for 3D bone tissue engineering," *Journal of Tissue Engineering and Regenerative Medicine*, vol. 3, no. 5, pp. 398–404, 2009.

[13] X. Miao, L.-P. Tan, L.-S. Tan, and X. Huang, "Porous calcium phosphate ceramics modified with PLGA-bioactive glass," *Materials Science and Engineering C*, vol. 27, no. 2, pp. 274–279, 2007.

[14] V. Guarino and L. Ambrosio, "The synergic effect of polylactide fiber and calcium phosphate particle reinforcement in poly ε-caprolactone-based composite scaffolds," *Acta Biomaterialia*, vol. 4, no. 6, pp. 1778–1787, 2008.

[15] A. E. Watts, A. J. Nixon, M. G. Papich, H. D. Sparks, and W. S. Schwark, "In vitro elution of amikacin and ticarcillin from a resorbable, self-setting, fiber reinforced calcium phosphate cement," *Veterinary Surgery*, vol. 40, no. 5, pp. 563–570, 2011.

[16] K. J. L. Burg, S. Porter, and J. F. Kellam, "Biomaterial developments for bone tissue engineering," *Biomaterials*, vol. 21, no. 23, pp. 2347–2359, 2000.

[17] S. Yang, K.-F. Leong, Z. Du, and C.-K. Chua, "The design of scaffolds for use in tissue engineering. Part I: traditional factors," *Tissue Engineering*, vol. 7, no. 6, pp. 679–689, 2001.

[18] K. F. Leong, C. M. Cheah, and C. K. Chua, "Solid freeform fabrication of three-dimensional scaffolds for engineering replacement tissues and organs," *Biomaterials*, vol. 24, no. 13, pp. 2363–2378, 2003.

[19] J. Russias, E. Saiz, R. K. Nalla, K. Gryn, R. O. Ritchie, and A. P. Tomsia, "Fabrication and mechanical properties of PLA/HA composites: a study of *in vitro* degradation," *Materials Science and Engineering C*, vol. 26, no. 8, pp. 1289–1295, 2006.

[20] R. Z. Le Geros, "Calcium phosphate-based osteoinductive materials," *Chemical Reviews*, vol. 108, no. 11, pp. 4742–4753, 2008.

[21] C. E. Wen, Y. Yamada, K. Shimojima, Y. Chino, H. Hosokawa, and M. Mabuchi, "Compressibility of porous magnesium foam: dependency on porosity and pore size," *Materials Letters*, vol. 58, no. 3-4, pp. 357–360, 2004.

[22] L. L. Hench and J. M. Polak, "Third-generation biomedical materials," *Science*, vol. 295, no. 5557, pp. 1014–1017, 2002.

[23] D. Williams, "Benefit and risk in tissue engineering," *Materials Today*, vol. 7, no. 5, pp. 24–29, 2004.

[24] V. Guarino, F. Causa, and L. Ambrosio, "Bioactive scaffolds for bone and ligament tissue," *Expert Review of Medical Devices*, vol. 4, no. 3, pp. 405–418, 2007.

[25] D. W. Hutmacher, J. T. Schantz, C. X. F. Lam, K. C. Tan, and T. C. Lim, "State of the art and future directions of scaffold-based bone engineering from a biomaterials perspective," *Journal of tissue engineering and regenerative medicine*, vol. 1, no. 4, pp. 245–260, 2007.

[26] L. Gerhardt and A. R. Boccaccini, "Bioactive glass and glass-ceramic scaffolds for bone tissue engineering," *Materials*, vol. 3, pp. 3867–3910, 2010.

[27] H. H. K. Xu, S. Takagi, J. B. Quinn, and L. C. Chow, "Fast-setting calcium phosphate scaffolds with tailored macropore formation rates for bone regeneration," *Journal of Biomedical Materials Research A*, vol. 68, no. 4, pp. 725–734, 2004.

[28] M. Alshaaer, H. Cuypers, H. Rahier, and J. Wastiels, "Production of monetite-based Inorganic Phosphate Cement (M-IPC) using hydrothermal post curing (HTPC)," *Cement and Concrete Research*, vol. 41, no. 1, pp. 30–37, 2011.

[29] C. Wenchuan, Z. Hongzhi, D. W. Michael, B. Chongyun, and H. H. K. Xu, "Umbilical cord stem cells released from alginate-fibrin microbeads inside macroporous and biofunctionalized calcium phosphate cement for bone regeneration," *Acta Biomaterialia*, vol. 8, no. 6, pp. 2297–2306, 2012.

[30] M. Alshaaer, H. Cuypers, G. Mosselmans, H. Rahier, and J. Wastiels, "Evaluation of a low temperature hardening Inorganic Phosphate Cement for high-temperature applications," *Cement and Concrete Research*, vol. 41, no. 1, pp. 38–45, 2011.

[31] J. Rouwkema, N. C. Rivron, and C. A. van Blitterswijk, "Vascularization in tissue engineering," *Trends in Biotechnology*, vol. 26, no. 8, pp. 434–441, 2008.

[32] M. Lovett, K. Lee, A. Edwards, and D. L. Kaplan, "Vascularization strategies for tissue engineering," *Tissue Engineering B*, vol. 15, no. 3, pp. 353–370, 2009.

[33] X. Shi, B. Sitharaman, Q. P. Pham et al., "Fabrication of porous ultra-short single-walled carbon nanotube nanocomposite scaffolds for bone tissue engineering," *Biomaterials*, vol. 28, no. 28, pp. 4078–4090, 2007.

[34] C. K. Kuo and P. X. Ma, "Ionically crosslinked alginate hydrogels as scaffolds for tissue engineering. Part 1: structure, gelation rate and mechanical properties," *Biomaterials*, vol. 22, no. 6, pp. 511–521, 2001.

[35] J. L. Drury, R. G. Dennis, and D. J. Mooney, "The tensile properties of alginate hydrogels," *Biomaterials*, vol. 25, no. 16, pp. 3187–3199, 2004.

[36] C. J. Damien and J. R. Parsons, "Bone graft and bone graft substitutes: a review of current technology and applications," *Journal of Applied Biomaterials*, vol. 2, no. 3, pp. 187–208, 1991.

[37] Y. Lei, B. Rai, K. H. Ho, and S. H. Teoh, "*In Vitro* degradation of novel bioactive polycaprolactone-20% tricalcium phosphate composite scaffolds for bone engineering," *Materials Science and Engineering C*, vol. 27, no. 2, pp. 293–298, 2007.

[38] C. R. Kothapalli, M. T. Shaw, J. R. Olson, and M. Wei, "Fabrication of novel calcium phosphate/poly(lactic acid) fiber composites," *Journal of Biomedical Materials Research B*, vol. 84, no. 1, pp. 89–97, 2008.